Brain network interconnectivity dynamics explain metacognitive differences in listening behavior

Mohsen Alavash*, Jonas Obleser*

Department of Psychology, University of Lübeck, 23562 Lübeck, Germany

Center for Brain, Behavior, and Metabolism, University of Lübeck, 23562 Lübeck, Germany

Abstract

Complex auditory scenes pose a challenge to attentive listening, rendering listeners slower and more uncertain in their perceptual decisions. How can we explain such behaviors from the dynamics of cortical networks that pertain to control of listening behavior? We here follow up on our hypothesis that listener's ability to flexibly adapt to challenging listening situations is supported by modular reconfiguration of auditory-control networks in a sample of N=40 participants who underwent resting-state and task fMRI. Individual titration of a spatial selective auditory attention task maintained an average accuracy of ~70% but yielded considerable inter-individual differences in listeners' response speed and reported confidence. Whole-brain network modularity increased from rest to task by reconfiguring auditory, cinguloopercular, and dorsal attention networks. Specifically, interconnectivity between nodes of auditory network and ciguloopercular network decreased mainly in suramarginal gyri, anterior insular, and anterior-/mid-cingulate cortices. In addition, interconnectivity between nodes of dorsal attention network and cinguloopercular network increased in parietal lobules and frontal eye-fields. These interconnectivity dynamics were predictive of individual differences in response speed and confidence. Our findings uncover the behavioral relevance of functional crosstalk between sensory and attentional-control networks under uncertainty and suggest two functionally dissociable cortical networked systems that shape metacognitive differences between individuals.

Keywords Adaptive listening behavior, individual metacognitive differences, confidence, cinguloopercular network, dorsal attention network

**Corresponding author* Mohsen Alavash, Jonas Obleser; Maria-Goeppert-Str. 9a, 23562 Lübeck, Germany mohsen.alavash@uni-luebeck.de; jonas.obleser@uni-luebeck.de

Significance Statement

The ability to communicate in challenging listening situations varies not only objectively between individuals. Listeners also differ notably in their subjective perceptual confidence. Using fMRI and a challenging selective pitch discrimination task, we here show that this variability in metacognitive aspect of listening behavior manifests on cortical level by modular reconfiguration of brain networks. This adaptive reconfiguration entails sensory and attentional-control networks. Importantly, task-related modulation of interconnectvity between cinguolopercular network and each auditory and dorsal attention network predict individual differences in response speed and confidence. This suggests two dissociable cortical networked systems that shape individual listening behavior under uncertainty. The interconnectivity dynamics uncovered here can explain for individuals' differences in evaluation of their own metacognitive perception during listening. This promises new opportunities to better understand and intervene on deficits of auditory perception such as age-related sensorineural hearing loss or auditory hallucinations.

Introduction

In complex auditory scenes, attending only to what we want to hear can be a challenging task, making our listening prone to errors and uncertainties. Listening as such not only hinges on the auditory fidelity, but also requires brain networks associated with directing, switching, and maintaining auditory attention (Shinn-Cunningham, 2008; Hill and Miller, 2010). In recent years there has been growing interest in studying listening as a trait-like behavior, as individuals differ substantially in utilizing cognitive strategies to control their auditory attention (Peelle, 2017; Shinn-Cunningham, 2017; Waschke et al., 2017; Tune et al., 2021). Nevertheless, the neural underpinnings of this inter-individual variability are poorly understood.

Previous functional magnetic resonance imaging (fMRI) studies have associated auditory attention with regions overlapping with temporal and dorsal-parietal cortices (Puschmann et al., 2017; Shiell et al., 2018) as well as cinguloopercular and insular cortex in challenging listening tasks (Eckert et al., 2009; Wild et al., 2012; Erb et al., 2013; Vaden et al., 2019). In addition, as it has been reviewed elsewhere, when listeners selectively focus their auditory attention to a particular location, cortical areas overlapping with well-known visuospatial attention networks are more active as compared to when not listening (Lee et al., 2014).

In parallel, functional connectivity studies have identified large-scale brain networks involved in cognitively demanding tasks which include a cinguloopercular/insular network (Dosenbach et al., 2008; Menon and Uddin, 2010; Sadaghiani and D'Esposito, 2015), a frontoparietal network (Seeley et al., 2007; Marek and Dosenbach, 2018), and a dorsal attention network (Fox et al., 2006; Szczepanski et al., 2013). Surprisingly, whether and how these attentional control networks support adaptive listening behavior has remained somewhat understudied and incompletely understood.

The emerging field of network neuroscience provides the theoretical basis to address this question (Bassett and Sporns, 2017). Within this framework, it has been shown that most of the variance in the configuration of brain networks arise from inter-individual variability rather than task contexts (Gratton et al., 2018). Along these lines of research, our previous fMRI study provided a large-scale brain network account of adaptive listening behavior (Alavash et al., 2019). Specifically, we were able to explain individual adaptation to a challenging listening task with concurrent speech by reconfiguration of a brain network composed of auditory, cinguloopercular, and ventral attention nodes toward increased modular segregation during the task relative to resting-state baseline.

However, an often understudied and thus not explained aspect of human adaptive perception and communication lies in the subjective assessment of one's own perceptual performance. Many neuroimaging studies of auditory cognition, including our own, have measured behavior only objectively using individuals' response accuracy (also labelled as "type I" perceptual decisions; Galvin et al., 2003) and, sometimes, speed. Challenging listening situations naturally introduce uncertainties to individual's evaluation of own auditory perception, thus confidence in listening (secondary to listening accuracy). This subjective evaluation can be viewed as a second-order measure of listening behavior, also referred to as "type II" decision (see above ref.). Such subjective reports can vary markedly from objective measures of listening behavior (Wostmann et al., 2021). Thus, one important question is whether and how brain network reconfiguration regulates or contributes to individual's confidence in listening under uncertainty. Knowing the role of cinguloopercular and insular networks in listening under challenging situations and more generally in performance monitoring and interoception (Fleming and Dolan, 2012; Uddin, 2015; Rouault et al., 2018), it is plausible to associate these interoceptive networks with subjective evaluation of own listening performance under uncertainty, that is, with a variant of "metalistening" (but see Fleming et al., 2012b).

In the light of our previous work (Alavash et al., 2019), we here aim at identifying and characterizing auditory-attentional control networks by studying how modular configuration of whole-brain networks changes from rest to a challenging selective pitch discrimination task. The present study thus leverages the degree and direction of network dynamics and asks two questions: (1) how are large-scale functional connectivity networks being reconfigured to support selective listening under uncertainty, and (2) how can such a reconfiguration explain individual differences not only in objective, but in subjective measures of listening behavior?

Results

We measured brain activity using fMRI in a sample of healthy young adults (N = 40; 18–32 y old) and constructed large-scale cortical connectivity networks (Fig. S1). This was done separately for a first 10-minute period of eyes-open resting-state measurement and for a second, ensuing 1-hour period where individuals performed an adaptive auditory attention task, namely selective pitch-discrimination (Fig. 1). The listening task was identical to the one used in our previous EEG study (Wöstmann et al., 2019). In brief, participants were presented with two concurrent tone sequences inside MRI scanner, one of which was always presented in front and the other in left or right in a block-wise fashion (Fig.1A). The virtual spatialization of sounds was achieved using individually selected head-related transfer functions (HRTFs; see SI Appendix for details).

On each trial, prior to tone presentation, an auditory spatial cue prompted the participants to attend to one of the tone sequences and to judge the pitch difference (increase/decrease) in the to-be-attended sequence. Listeners also reported their confidence in own decision (high/low; Fig. 1B). The pitch difference was individually titrated throughout the experiment using an adaptive tracking procedure to retain the listeners' overall accuracy at ~70%. This procedure made sure that the task was equally challenging enough, and in turn yielded considerable inter-individual variability in listeners' response speed and confidence (Fig. 1C).

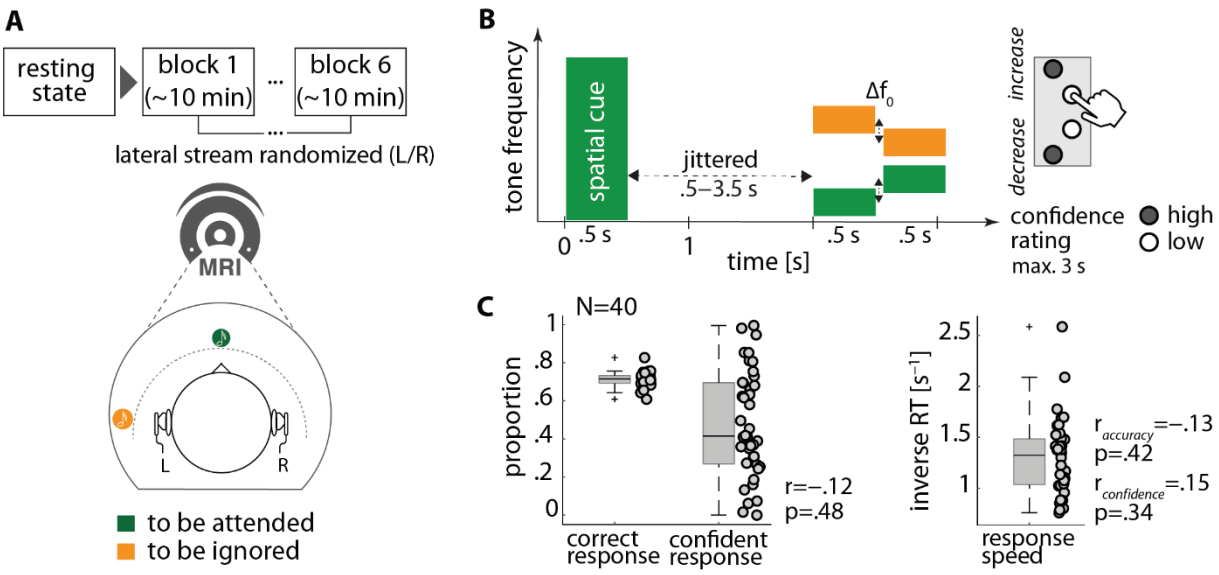

Figure 1. Listening paradigm and individuals' behavior. (A) FMRI measurement. Following 10-min eyes-open resting state, participants performed six blocks of purely auditory selective pitch discrimination task. During the task, two competing tone sequences were presented using in-ear headphones. The virtual spatialization of sounds was achieved using individually selected head-related transfer functions (HRTFs). One tone sequence was always presented at front and the other was switched between left and right over task blocks (left/right order randomized across participants). (B) Trial structure. Each trial started by presentation of a broadband auditory cue (0–10 kHz; 0.5 s) followed by a jittered silent interval. Next, two tone sequences, each consisting of two brief (0.5 s) complex tones, were presented at different locations (front, left, or right). Fundamental frequencies of low-frequency tones within each sequence were fixed at 177 and 267 Hz. Frequencies of high-frequency tones were titrated throughout the experiment (Δf_0: tracking parameter). Participants had to judge whether the target tone sequence at the cued location had increased or decreased in pitch. Participants also reported their confidence in own decision (high: outer buttons; low: inner buttons). (C) Individuals' listening behavior. Listeners' behavior was measured both objectively and subjectively using response accuracy, speed (i.e., inverse reaction time; 1/RT), and confidence rating. *Box plots*. The central line indicates the median, and the bottom and top edges of the box indicate the 25th and 75th percentiles, respectively. The whiskers extend to the most extreme data points not considered outliers. The outliers are marked by '+' symbol. Individuals showed considerable variability in their listening behavior, notably in response speed and confidence. The behavioral measures were uncorrelated across listeners (insets).

Guided by our previous fMRI study on brain network account of spatial selective auditory attention (Alavash et al., 2019), we predicted that during the task brain networks would reconfigure toward higher functional segregation as quantified by network modularity. Importantly, we asked if a reconfiguration as such can explain inter-individual variability in listening confidence independent form listening accuracy. To this end, we used (generalized) linear mixed effects models to examine the influence of the experimental conditions and brain network dynamics on listeners' single-trial behavior measured using response accuracy, speed, and confidence.

High inter-individual variability in response speed and confidence during selective pitch discrimination task

The average pitch difference between the consecutive tones (i.e., the stimulus parameter tracked per listener adaptively; Fig. 1B, Δf_0) was 0.84 semitones (± 0.69 semitones between-subject SD). As intended, the resulting accuracy (average proportion correct) was 71% (± 3.6% between-subject SD).

Notably, as illustrated in Fig.1C, listeners showed considerable inter-individual variability in their response speed (mean ± SD response speed = 1.23 ± 0.37s^{-1}; coefficient of variation = 0.3) and in their confidence (average proportion and SD of 'confident' responses = 48% ± 28%; coefficient of variation = 0.58).

Lending plausibility to the behavioral results obtained, single-trial listening behavior confirmed the beneficial effect of pitch difference on listeners' behavior, i.e., the larger the pitch difference, better the behavioral performance (accuracy: odds ratio (OR) = 1.42, $p < 0.001$; speed: $\beta = 0.26$, $p < 0.01$; confidence: OR = 5.97, $p < 0.001$; Table S1-3). Listeners also showed better performance when the direction of the pitch change was congruent across the two tone sequences (accuracy: OR = 3.06, $p < 0.001$; confidence: OR = 1.2, $p < 0.001$; speed: $\beta = 0.07$, $p < 0.01$; Table S1-3). In addition, listeners were less confident when the to-be-attended tone sequence was presented in front compared with side (OR = 0.84, $p < 0.01$; Table S2). All of these effects were very well in line with the results we found in our previous EEG study in which the stimuli during the same task were presented in free field using loudspeakers (Wöstmann et al., 2019).

Of relevance to all further brain-behavior results, the three behavioral measures proved largely independent from each other and reliable. Only if they are sufficiently reliable, meaning that individual data on repeated tests correlate positively, any brain-behavior relation, which is the main scope here, can be interpreted in a meaningful way (Guggenmos, 2021).

First, proportion correct, response speed, and confidence were largely uncorrelated across listeners (Spearman's rho magnitude < 0.2, p-values > 0.3; Fig. 1C, insets), suggesting their unique roles in the translation of sensory information into perceptual decisions and ensuing behavior.

Second, using the individual data across six blocks of the task (96 trials per block), we calculated the reliability metric Cronbach's alpha (CA) for each measure. The result indicated relatively high reliability of each behavioral measure, particularly so for response speed and confidence (accuracy: CA = 0.58, speed: CA = 0.95, confidence: CA = 0.98).

Higher modularity of cortical networks during selective pitch discrimination task

Using the fMRI data, we first asked whether functional segregation of large-scale brain networks increases under auditory spatial selective attention. Accordingly, our main analysis started by comparing functional segregation of brain networks during the listening task relative to rest. The degree of functional segregation can be quantified using the graph-theoretical measure known as modularity which captures the decomposability of a network into subsystems (Fig. 2A) (Rubinov and Sporns, 2010) and has been suggested to support cognitive flexibility and adaptive behaviors (Bassett et al., 2010; Alavash et al., 2015a; Bertolero et al., 2018). Guided by our previous fMRI study (Alavash et al., 2019), we expected that brain network modularity would increase during the spatial selective pitch discrimination task relative to resting state.

Our network comparison revealed a significant increase in network modularity during the task relative to rest (permutation test; Cohen's d = 0.3, p = 0.02; Fig. 2B, left). Importantly, resting-state and listening task networks did not differ in their overall mean functional connectivity (Cohen's d = –0.01, p = 0.93; Fig. 2B, right). This emphasizes the importance of modular reconfiguration (i.e., change in network topology) in brain network adaptation to the current task context in contrast to a mere alteration in overall functional connectivity (change in correlation strength). This result was in good agreement with our previous study in which whole-brain network modularity increased during a dichotic listening task with concurrent speech (Alavash et al., 2019).

In an additional analysis, we investigated the correlation of brain connectivity and network modularity between resting state and listening task. Reassuringly, both measures were positively correlated across participants (connectivity: Spearman's rho = 0.5, $p < 0.01$; modularity: rho = 0.61, $p < 0.01$), supporting the idea that state- and trait-like determinants both contribute to individuals' brain network configurations (Geerligs et al., 2015). Lending generality to all further results, we did not find any significant difference in network modularity between attend left versus attend right (permutation test; d = 0.04, p = 0.5), or left versus front (d = 0.03, p = 0.75), or right versus front (d = 0.01, p = 0.86).

We next investigated whether reconfiguration of the whole-brain networks from rest to task can account for the inter-individual variability in listening behavior (Fig. 1C). To this end, using the same linear mixed effects model that revealed the beneficial effects of the pitch difference and congruency of the tone sequences on objective and subjective measures of behavior, we tested whether alteration in network modularity relative to rest could predict listeners' single-trial behavior. In our models, we also included whole-brain resting-state and task mean connectivity as between-subject covariates.

We found a significant interaction between individuals' whole-brain resting-state and task network modularity in predicting single-trial confidence ratings (OR = 1.12, $p < 0.01$). This interaction was driven by a negative relationship between task modularity and confidence for a group of individuals whose resting state modularity was lower than average (OR = 0.88, $p < 0.01$) and the absence of such a relationship for the other group showing resting modularity higher than average (OR = 0.97, p = 0.68). This result provided initial evidence that, at the whole-brain level, reconfiguration of network modules is most likely task-relevant, as it has the potential to explain individual differences in listeners' response confidence.

However, the effects of pitch difference, congruency of the tones, or role of the lateral stream (i.e., to-be-attended or to-be-ignored) on single-trial confidence ratings were not significantly modulated by whole-brain network modularity. More precisely, adding an interaction term between these experimental conditions and brain network modularity did not significantly improve the model fit (likelihood ratio tests; pitch difference: $\chi2 = 0.54$, p = 0.45; congruency: $\chi2 = 0.01$, p = 0.92; role of the lateral stream: $\chi2 = 3.2$, p = 0.07). Also, the interaction between rest and task modularity in predicting single-trial accuracy or response speed was not significant (accuracy: OR = 1.02, p = 0.79; speed: $\beta = -0.02$, p = 0.35).

Following the analysis rationale established in (Alavash et al., 2019), the following sections will explore the cortical origin of the modular reconfiguration outlined above: first, at the whole-brain level and second, at a subnetwork level in more detail. In the final section of the results, we will illustrate the behavioral relevance of these network dynamics at the individual level.

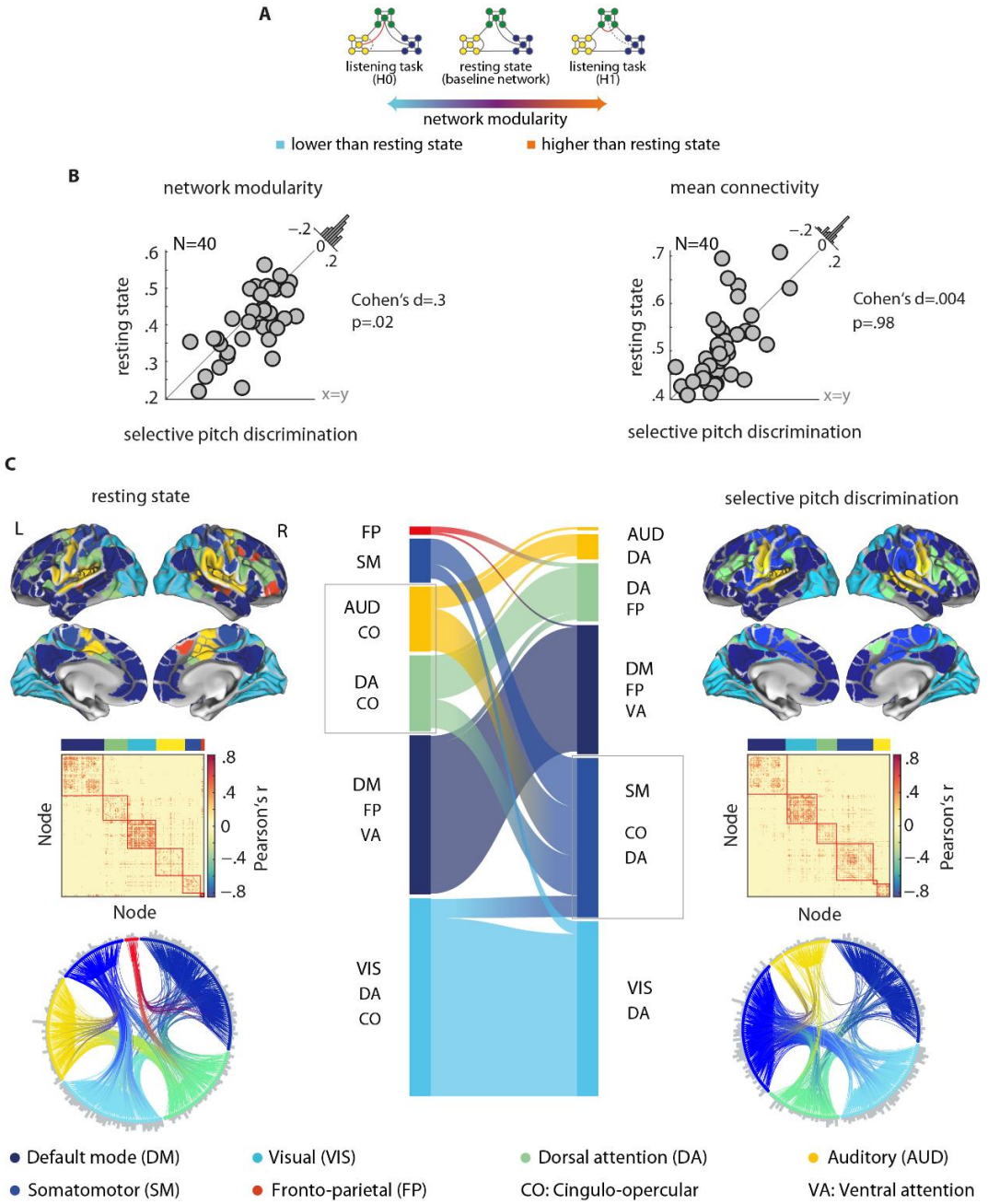

Figure 2. Reconfiguration of whole-brain network under the listening task relative to resting state. (A) Two possible network reconfigurations (i.e., left/right toy graphs compared to middle graph). Higher functional segregation is characterized by an increase in network modularity, a measure that quantifies grouping of nodes into relatively dense subsystems (here shown in distinct colors), which are sparsely interconnected. Toward higher functional segregation, the hypothetical baseline network loses the shortcut between the blue and green module (dashed link). Instead, within the green module, a new connection emerges (red link). (B) During the listening task, whole-brain mean connectivity was not significantly different than rest (left plot), whereas network modularity significantly increased (right plot). Histograms show the distribution of the change (task minus rest) across all 40 participants. (C) Whole-brain resting-state network decomposed into distinct modules shown in different colors. The network modules are visualized on the cortical surface, within the functional connectivity matrix, and on the connectogram using a consistent color scheme. Modules are identified according to their node labels as in Gordon parcellation. Group-level modularity partition was obtained using graph-theoretical consensus community detection. Gray peripheral bars around the connectograms indicate the number of connections per node. Flow diagram in the middle illustrates the reconfiguration of brain network modules from resting state (left) to the listening task (right). Modules are shown in vertical boxes with their heights corresponding to their connection densities. The streamlines illustrate how nodes belonging to a given module during resting state change their module membership under the listening task.

Reconfiguration of auditory and attentional-control networks during selective pitch discrimination task

Fig. 2C provides a comprehensive overview of group-level brain networks, functional connectivity maps, and the corresponding connectograms (circular diagrams) during resting state (Fig. 2C, Left) and during the listening task (Fig. 2C, Right). In Fig. 2, cortical regions defined based on Gordon parcellation (Gordon et al., 2016) are grouped and color coded according to their module membership determined using the graph-theoretical consensus community detection algorithm (see SI Appendix for details). When applied to the resting-state data in our sample (N = 40), the algorithm decomposed the group-averaged whole-brain network into six modules (Fig. 2C, Left). The network module with the highest number of nodes largely overlapped with the known default mode network (Fig. 2C, dark blue). In the light of our previous study (Alavash et al., 2019) our investigation was particularly focused on the module comprising mostly auditory nodes and a number of cinguloopercular nodes (Fig. 2C, yellow). For simplicity, similar to (Alavash et al., 2019) we will refer to this module as the auditory module. Additional network modules included visual (Fig. 2C, cyan), somatomotor (Fig. 2C, light blue), dorsal attention (Fig. 2C, green), and frontoparietal module (Fig. 2C, red).

Fig. 2C shows how the configuration of the whole-brain network changed from rest to task. This network flow diagram illustrates whether and how cortical nodes belonging to a given network module during resting state (Fig. 2C, Left) changed their module membership during the listening task (Fig. 2C, Right). The streamlines tell us how the nodal composition of network modules changed, indicating a functional reconfiguration. According to the streamlines, the auditory and dorsal attention modules showed the most prominent reconfiguration (Fig. 2C, yellow and green modules, respectively), while the other modules underwent only moderate reconfigurations. This reconfiguration is very well in line with the results we found in our previous study, in which N = 49 participants completed resting state followed by selective listening task with concurrent speech.

Specifically, here this reconfiguration can be summarized by a nodal "branching" of the auditory module during selective pitch discrimination (Fig. 2C, left gray box) accompanied by formation of a module comprised of cinguloopercular, somatomotor, dorsal attention, and visual nodes. Knowing the pure auditory nature of the listening task here, the less prominent changes in visual nodes deem unlikely to be behaviorally relevant to task performance. To rule this out, for our brain-behavior models, we conducted control analyses in which main predictors were derived from visual or somatomotor networks (see section *Control analyses*). Taken together, we have observed a reconfiguration of the whole-brain network that is dominated by alterations across auditory, cinguloopercular, and dorsal attention nodes.

Accordingly, similar to (Alavash et al., 2019) we next identified the cortical origin of these network dynamics based on the underlying functional parcellation (Gordon et al., 2016). The identified subnetwork entails auditory, cinguloopercular, and dorsal attention nodes. We will refer to this large-scale cortical subnetwork collectively as the auditory attentional-control network. This subnetwork encompasses 96 nodes (of 333 whole-brain nodes). According to Fig. 2C, this subnetwork is in fact a conjunction across all auditory, cingulo-opercular, and dorsal attention nodes, irrespective of their module membership. For the purpose of a more transparent illustration, the cortical map of the auditory attentional-control network is visualized in Fig. 3A.

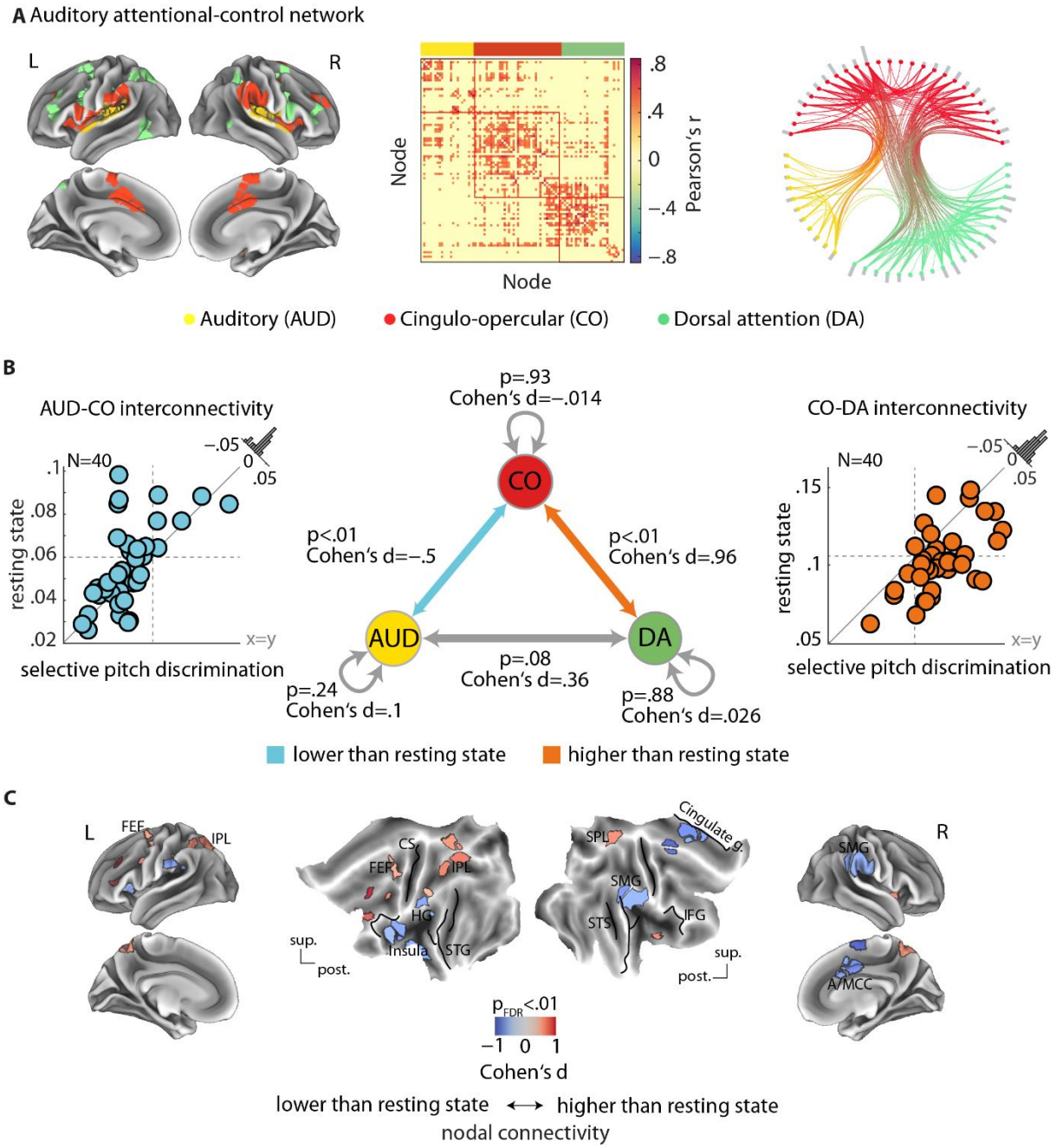

Figure 3. Modulation of connectivity across auditory and attentional-control networks. (A) The auditory attentional-control network composed of auditory (AUD), cinguloopercular (CO), and dorsal attention (DA) nodes. Nodes are identified according to their labels in Gordon parcellation. The correlation structure and connection pattern across these nodes are illustrated by group-level functional connectivity matrix and the connectogram (circular diagram), respectively. Gray peripheral bars around the connectogram indicate the number of connections per node. (B) Modulation of cinguloopercular connectivity with auditory and dorsal attention networks during the listening task. From rest to task, AUD-CO mean connectivity decreased (left plot), whereas CO-DA connectivity increased (right plot). Mean connectivity across nodes within each network or between auditory and dorsal attention networks did not change significantly (middle graph, gray arrows). Histograms show the distribution of the change (task minus rest) across all 40 participants. (C) Modulation of nodal connectivity across the auditory attentional-control network. Nodal connectivity (also known as strength) was quantified as the sum of correlation values per node. The result was compared between task and rest per node using paired permutation tests and corrected foe multiple comparison across nodes (FDR correction). Nodes showing significant decrease in their connectivity during the listening task overlapped with bilateral supramarginal gyri, left anterior insula, and right anterior cingulate cortices. Nodes showing significant increase in their connectivity overlapped with superior parietal/intraparietal lobule (SPL/IPL) and frontal eye fields (FEF).

Modulation of interconnectivity across the auditory attentional-control network

Despite significant increase in whole-brain network modularity during the listening task relative to rest (Fig. 2B) neither mean connectivity nor modularity of the auditory attentional-control network was significantly different than rest (connectivity: $d = 0.04$, $p = 0.79$; modularity: $d = -0.21$, $p = 0.13$). Nevertheless, it is still possible that different connectivity patters across the auditory attentional-control network emerge such that the net modulation as captured by mean connectivity cancels out. We thus investigated whether and how connectivity within and between auditory, cinguloopercular, and dorsal attention nodes is modulated during the listening task relative to rest.

The result is visualized in Fig. 3B. We found two different patterns of connectivity modulation across the auditory attentional-control network. First, from rest to task, mean connectivity between auditory and cinguloopercular network (AUD-CO) was decreased significantly (Cohen's $d = -0.5$, $p < 0.01$; Fig. 3B, Left). Second, mean connectivity between cinguloopercular and dorsal attention network (CO-DA) increased significantly (Cohen's $d = 0.96$, $p < 0.01$; Fig. 3B, Right). In addition, connectivity between auditory and dorsal attention network was increased, but the degree of this modulation did not reach the significance level (Cohen's $d = 0.36$, $p = 0.08$; Fig. 3B, Bottom).

Notably, mean connectivity within auditory or cinguluopercular or dorsal attention network was not significantly different that rest (Fig. 3B, gray self-connections). This observation speaks to the potency of functional crosstalk between auditory and attentional-control networks to regulate or contribute to metacognitive aspect of listening behavior.

Interestingly, AUD-CO connectivity and CO-DA connectivity were uncorrelated across participants under both rest and task (rest: rho=–.14, p=.4, task: rho=–.03, p=.86), which suggests two dissociable large-scale networked systems shaping adaptive listening behavior under uncertainty.

Next, we conducted a nodal analysis to delineate the cortical regions that drive the modulation of interconnectivity across the auditory attentional-control network. To this end, we used a simple graph-theoretical measure—namely, nodal connectivity (also known as nodal strength)—defined as the sum of each node's connection weights. Based on permutation tests to compare nodal connectivity between rest and task, we found that connectivity of mainly supramarginal gyri, anterior insular, and anterior/mid-cingulate cortices was significantly decreased during the selective pitch discrimination task relative to rest ($-1 <$ Cohen's $d < -0.53$, $p < 0.01$, false discovery rate (FDR)-corrected for multiple comparisons across nodes; Fig. 3C, blue). In addition, we found significant increase in connectivity of cortical nodes overlapping with parietal lobules and frontal eye-fields ($0.43 <$ Cohen's $d < 1$, $p < 0.01$; Fig. 3C, red).

Interconnectivity of auditory attentional-control network predicts metacognitive aspects of listening behavior

As Fig. 3B shows, listeners clearly showed inter-individual variability in the degree and direction of modulation in AUD-CO and CO-DA interconnectivity. Thus, we next investigated whether these variabilities could explain inter-individual variability in listening behavior (Fig. 1C). To this end, we tested the direct and interactive effects of individual mean interconnectivity during rest and task on single-trial response accuracy, speed, or confidence. These are the same linear mixed-effects models based on which the beneficial effects of pitch difference and congruency on behavior was reported earlier.

The brain-behavior relationships were tested in separate models for each AUD-CO and CO-DA network pairs. In each model, brain regressors were entered as between-subject covariates. In our models we controlled for activity level of each auditory, cinguloopercular, and dorsal attention network by including mean beta estimates derived from nodal activation analysis (Fig. S2) as additional between-subject covariates.

First, we found a significant main effect of AUD-CO interconnectivity on listeners' response speed ($\beta = 0.07$, $p < 0.001$; Fig. B; Table S1). This result indicates that, higher AUD-CO interconnectivity promoted faster decisions during the selective pitch discrimination task. In addition, we found that AUD-CO interconnectivity predicted listeners' response confidence, but only in those individuals whose resting-state AUD-CO interconnectivity was lower than average. Statistically, this surfaced as a significant interaction between resting-state AUD-CO interconnectivity and connectivity between the same network pair during the listening task in predicting single-trial confidence rating ($OR = 0.92$, $p < 0.05$; Fig 4A; see Table S2 for details). This result indicates that, among individuals with lower-than-average resting-state AUD-CO interconnectivity, higher AUD-CO connectivity during task was associated with higher proportion of confident responses (Fig. 4A, Left). The main effect of AUD-CO interconnectivity on response confidence was not significant ($OR = 1.07$, $p = 0.1$).

Second, dynamics of CO-DA interconnectivity predicted individual differences in both response speed and confidence (Fig. 5). Specifically, we found a significant interaction between CO-DA interconnectivity during rest and during task in predicting single-trial response speed ($\beta = 0.04$, $p < 0.05$; Fig. 5B; Table S3). This interaction indicates that, the behavioral relevance of CO-DA connectivity was conditional on individual resting-state connectivity: for listeners with resting-state connectivity lower than average, lower connectivity predicted faster responses, and for listeners with resting-state connectivity higher than average, higher connectivity predicted faster responses. In addition, a similar statistical pattern was found in predicting single-trial confidence rating ($OR = 1.18$, $p < 0.001$; Fig. 5A; Table S4). Note that in our data response confidence and speed were uncorrelated across listeners (Fig. 1C, insets). The main effect of CO-DA interconnectivity on response speed or confidence was not significant (speed: $\beta = 0.001$, $p = 0.98$; confidence: $OR = 0.96$, $p = 0.47$).

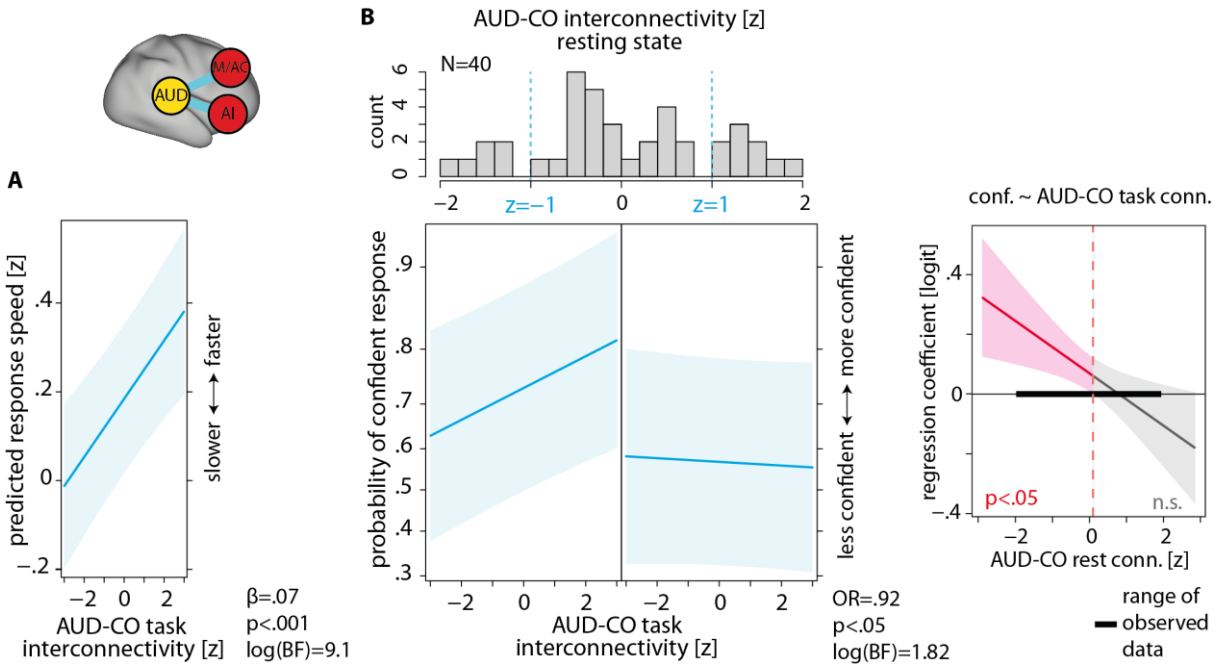

Figure 4. Prediction of individual listening behavior from dynamics of auditory-cinguloopercular interconnectivity. (A) Prediction of single-trial response speed from mean AUD-CO interconnectivity during the selective pitch discrimination task. Across listeners, higher AUD-CO interconnectivity predicted faster responses during the task (β = 0.07, p < 0.001, log-BF = 9.1). (B) Interaction between mean AUD-CO interconnectivity derived from resting state and the same connectivity under the selective pitch discrimination task predicted how confident individual listeners were in their responses (OR = 0.92, p < 0.05, log-BF = 1.82). For visualization purpose only, individuals were grouped according to their standardized mean resting state AUD-CO interconnectivity. Each correlation plot corresponds to one group of individuals. Distribution of resting state mean interconnectivity is shown by the top histogram. Solid blue lines indicate linear regression fit to the data when resting state interconnectivity held constant at the group mean (dashed blue line in histogram). *Johnson-Neyman plot.* To explore the interaction effect, the regression coefficient corresponding to the prediction of single-trial confidence ratings from AUD-CO interconnectivity under task is plotted at different values of the moderator (i.e., rest interconnectivity). The range of the values of the moderator in which the slope is significant is illustrated in red. Experimental variables including single-trial pitch differences, congruency of tone sequences, and location of spatial cue have been accounted for in the models. Shaded blue areas show two-sided parametric 95% CI. β: Slope parameter estimate from linear mixed-effect model. *OR*: odds ratio parameter estimate from generalized linear mixed-effects model. *M/AC*: Mid-/anterior cingulate. *AI*: Anterior insula.

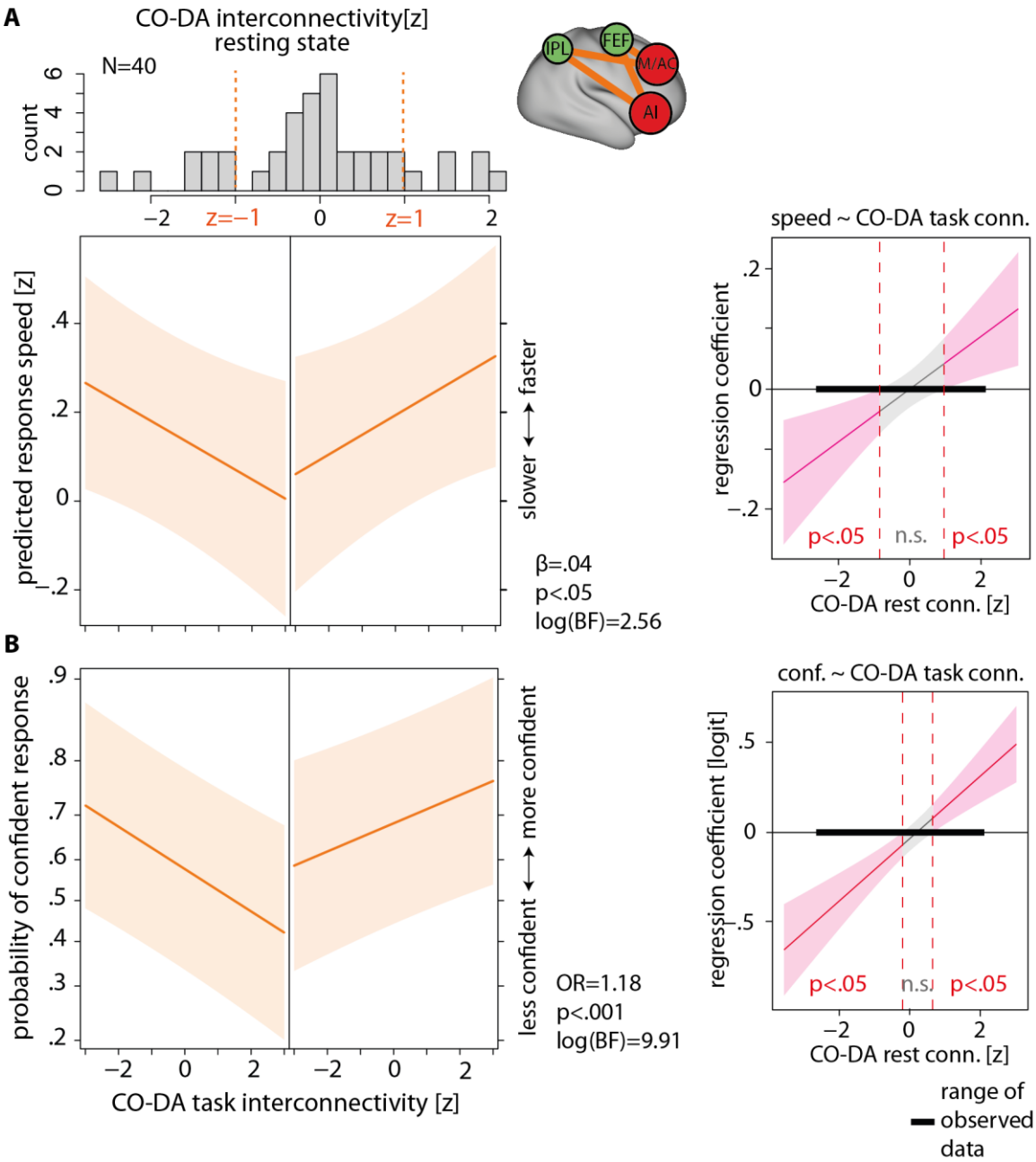

Figure 5. Prediction of individual listening behavior from dynamics of interconnectivity between cinguloopercular and dorsal attention network. (A) Interaction between mean CO-DA interconnectivity derived from resting state and task predicted how fast individual listeners were in their responses ($\beta = 0.04$, $p < 0.05$, log-BF = 2.56). For visualization purpose only, individuals were grouped according to their standardized mean CO-DA resting state interconnectivity. Each correlation plot corresponds to one group of individuals. Distribution of resting state mean interconnectivity is shown by the top histogram. Solid orange lines indicate linear regression fit to the data when resting state connectivity held constant at the group mean (dashed orange line in histogram). *Johnson-Neyman plot.* To explore the interaction effect, the slope of the regression line predicting single-trial response speed from CO-DA interconnectivity under task is plotted at different values of the moderator (i.e., rest interconnectivity). The range of the values of the moderator in which the slope is significant is illustrated in red. (B) Interaction between mean CO-DA interconnectivity derived from resting state and the same connectivity under the selective pitch discrimination task predicted how confident individual listeners were in their responses (OR = 1.18, $p < 0.001$, log-BF = 9.9). Data visualization is the same as in A, but here the dependent variable is single-trial response confidence. Experimental variables including single-trial pitch differences, congruency of tone sequences, and location of spatial cue have been accounted for in the models. Shaded orange areas show two-sided parametric 95% CI. β: Slope parameter estimate from linear mixed-effect model. *OR*: odds ratio parameter estimate from generalized linear mixed-effects model. *M/AC*: Mid-/anterior cingulate. *AI*: Anterior insula. *FEF*: Frontal eye-fields. *IPL*: Inferior parietal lobule.

Control analysis: Can activity or connectivity of other networks predict listeners' behavior?

Our findings illustrate that dynamics of interconnectivity across the auditory attentional-control network could partly explain individual differences in listening behavior. These dynamics were expressed as the interaction between resting-state and task mean connectivity between network pairs defined using average Pearson correlations, a commonly used measure of functional connectivity. Accordingly, one question is, in how far the brain-behavior relations observed here are driven by changes in cortical activity level rather than changes in correlation strength. In addition, from rest to task, somatomotor and visual networks also underwent a moderate reconfiguration (Fig. 2C). Thus, another question is whether interconnectivity with somatomotor or visual network can predict listeners' behavior. Therefore, we conducted a set of control analyses to ensure that the brain-behavior findings are not trivial.

First, in all our brain-behavior models we accounted for individual mean cortical activity of each auditory, cinguloopercular, and dorsal attention network by including between-subject covariates of mean beta estimates derived from activation analysis (Fig. S2). The main effects of these predictors on behavior were not significant (Table S1-S4).

Second, we tested additional brain-behavior models in which the connectivity regressors were defined based on interconnectivity between each somatomotor or visual network with auditory, cingulopercular, or dorsal attention network. Identical to our main analysis, these models were tested separately for each network pair in predicting single-trial response confidence or speed. The results are provided in Table S5. We only found a significant main effect of connectivity between somatomotor and auditory network in predicting listeners' response confidence ($OR = 1.15$, $p < 0.01$). This result indicates that those listeners who were more confident in their responses showed stronger auditory-somatomotor interconnectivity.

Discussion

The main goal of our study was to explain inter-individual variability in selective listening behavior under uncertainty by dynamics of cortical networks pertain to control of auditory attention. First, by studying modular reconfiguration of brain networks from resting state to the selective pitch discrimination task, we identified the large-scale auditory attentional-control network. Next, across this network and on individual level, we found that performing the task modulated the interconnectivity between cinguloopercular and each auditory and dorsal attention network: while auditory-cinguloopercular connectivity significantly decreased, we found a significant increase in connectivity between cinguloopercular and dorsal attention network. The results obtained from brain-behavior linear mixed-effects models supported the functional significance of these interconnectivity dynamics. In sum, depending on individual's intrinsic resting-state interconnectivity, up-/down-regulation of the interconnectivity of these two networked systems could be beneficial to an individual's perceptual decision speed and confidence during adaptive listening behavior.

Metacognitive facets of adaptive listening behavior

The selective listening paradigm used in the present study allowed listeners to judge the direction of pith change in a to-be-attended auditory object clearly above chance (accuracy of ~70%) but left them uncertain about their own selective perceptual decisions, as reflected in an overall response confidence of around ~50%. Across listeners, the subjective assessment of own listening performance varied considerably, and so did listeners' response speed.

Accordingly, our listening paradigm illustrates a situation where each listener's first-order performance was high, but awareness about own perception varied considerably across listeners. This highlights an important dimension to the study of adaptive listening behavior which can be formalized within the scope of metacognition as "matacognitive performance", defined as the ability to introspect about the correctness of own thoughts and actions (Fleming et al., 2012a).

What neurocognitive process can explain this inter-individual variability in metacognition during adaptive listening (or second-order listening behavior)? Our findings suggest that this variability is partly related to individual differences in dynamics of two cortical networked systems, as illustrated in Fig. 6 and discussed below.

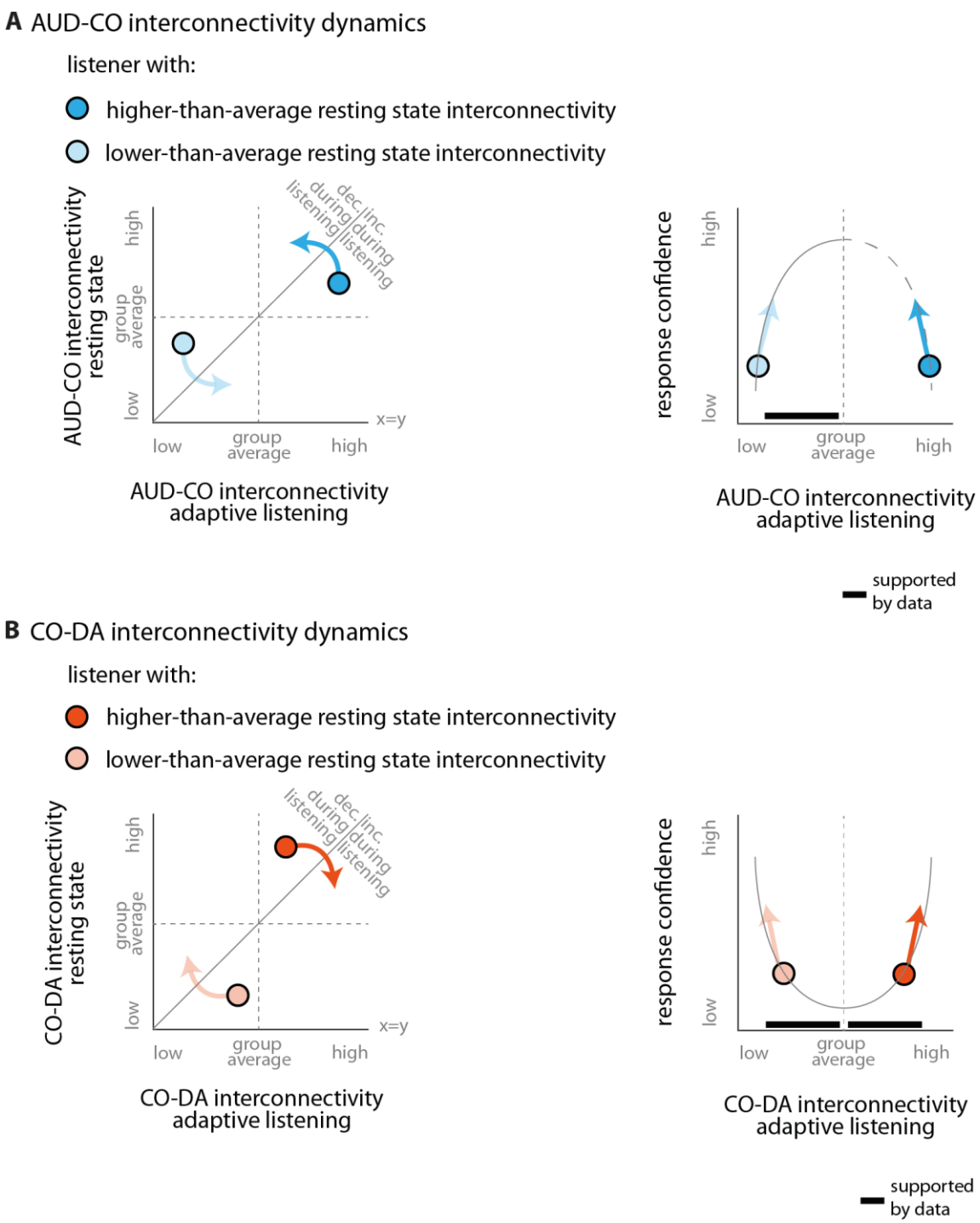

Figure 6. A putative dynamical repertoire of two large-scale cortical networked systems shaping human metacognitive performance during adaptive listening behavior. The interactions between rest and task interconnectivity of the auditory attentional-control network in predicting listeners' response confidence (Fig.4 and Fig. 5) imply quadratic relationships between response confidence and the interconnectivity dynamics. This is illustrated by dynamics of the solid circles that represent two individual listeners. For the individual listeners to behave more confident during adaptive listening (direction of arrows), interconnectivity of the two networked systems need to be regulated according to their individual intrinsic level. (A) Auditory-cinguloopercular (AUD-CO) interconnectivity around the group-average level during adaptive listening could be beneficial to individual listening confidence (cf. Fig. 4B). (B) Interconnectivity between cinguloopercular and dorsal attention networks (CO-DA) need to be up-/down-regulated according to the individual intrinsic interconnectivity (deviation from group-average) to support more confident listening (cf. Fig. 5). Note that a quadratic model does not necessarily require the data to be U-shaped. Other curvilinear relationships are possible, e.g., just one part of the parabola.

Interconnectivity of auditory and cinguloopercular networks communicates decision confidence during listening under uncertainty

Our first main finding was that higher connectivity between auditory and cinguloopercular network predicted faster responses during the listening task, and for listeners with lower-than-average resting state connectivity, higher auditory-cinguloopercular connectivity predicted more confident responses (Fig. 4). In our previous fMRI study, we similarly found that auditory-cinguloopercular connectivity significantly modulated during adaptive listening behavior, and higher functional segregation of a frontotemporal auditory-control network predicted more accurate and faster responses (Alavash et al., 2019).

Previous fMRI activation studies have consistently shown that cinguloopercular activity is predictive of word recognition during speech-in-noise experiments (Vaden et al., 2013; Eckert et al., 2016; Vaden et al., 2019). Recently, using a perceptual decision-making model, it has been shown that cinguloopercular activity contributes to criteria adjustments to optimize speech recognition performance (Vaden et al., 2022). In parallel, visual studies have shown that cinguloopercular network displays sustained activity during perceptual processing (Sestieri et al., 2014), with its activity level relating to the speed of stimulus detection (Coste and Kleinschmidt, 2016). These findings can be interpreted in the light of the proposed role for cinguloopercular cortex in performance monitoring, and more generally, adaptive control (Dosenbach et al., 2008; Power and Petersen, 2013; Neta et al., 2014; Neta et al., 2017).

Interestingly, previous work on neural correlates of metacognition during decision-making behavior support the role of frontal brain areas in subjective sense of decision confidence (Vaccaro and Fleming, 2018). Specifically, studies have found that explicit confidence estimates are tracked in cortical areas including medial/rostrolateral prefrontal cortex (De Martino et al., 2013; Hebart et al., 2016), and dorsal anterior cingulate cortex (Fleming et al., 2012b; Fleming et al., 2014). Additionally, it has been shown that medial prefrontal cortex is linked to inter- and intra-individual variation in explicit confidence estimates (Bang and Fleming, 2018). Direct evidence comes from an animal study in which authors identified the orbitofrontal cortex to be involved in confidence based behaviors (Kepecs et al., 2008). Thus, evaluation of own decision confidence during adaptive behaviors seems to critically rely on neural computations implemented across cingulate and prefrontal cortices.

Collectively, the functional overlap between cinguloopercular network being involved in adaptive control and frontal cortical areas representing decision confidence fits well with the idea of a domain-general role of cinguloopercular network in neural representation of metacognitive performance (Baird et al., 2013; Rouault et al., 2018; Rouault et al., 2023). Accordingly, one possible network mechanism underlying our finding could be that, cinguloopercular nodes detect, communicate, and integrate uncertainty into decision process according to ones' listening goal (cf. (Gordon et al., 2018)).

Interconnectivity of cinguloopercular and dorsal attention networks accounts for metacognitive performance during selective listening

Our second main finding was that, up-/down-regulation of interconnectivity between cinguloopercular and dorsal attention networks predicted listeners' response speed and confidence during the selective pitch discrimination task (Fig. 5). Selective attention, especially in visual and spatial domains, is known to recruit dorsal attention network (Corbetta et al., 2008; Petersen and Posner, 2012; Posner, 2012; Vossel et al., 2014). Neuroimaging studies have shown that spatial auditory attention recruits some of the same cortical regions as visuospatial attention (Lee et al.,

2014). Activation analysis of our data indeed supports the involvement of dorsal attention nodes in selective processing of the concurrent tones (Fig. S2D). In addition, it has been shown that cinguloopercular network is flexibly linked with dorsal attention network during visuospatial or memory search, respectively, consistent with the characterization of the cinguloopercular network as a domain-general task-control system (Sestieri et al., 2014). Studies in non-human animals have also associated the canonical nodes of the dorsal attention network, namely inferior parietal sulcus and supplementary frontal eye fields, to metacognitive performance during visual-spatial tasks (Kiani and Shadlen, 2009; Middlebrooks and Sommer, 2012).

Our findings add to the growing understanding of the cortical substrate of spatial selective auditory attention by illustrating that the functional crosstalk between cinguloopercular and dorsal attention network is behaviorally relevant to selective listening to the extent that it could partly explain individual differences in metacognition during listening behavior. This brain-behavior relationship was found as an interaction between rest and task CO-DA interconnectivity, in which the slope of the linear regression of response speed or confidence on CO-DA task interconnectivity was conditioned on individual's resting state interconnectivity. Since task and rest connectivity correlate across individuals (in the present study: Spearman's rho = 0.5, $p < 0.01$), this pattern suggests that the slope of the linear regression is not constant but depends on task connectivity itself. This would hypothetically imply a quadratic relationship (Fig. S3). Therefore, in a post-hoc analysis we additionally tested the main effect of the linear and quadratic trend (i.e., squared) of CO-DA task interconnectivity on behavior. We found a significant main effect of the quadratic term on response confidence (OR = 0.84, $p < 0.01$; Fig. S3). This result suggests a U-shape relationship between individual CO-DA interconnectivity and response confidence during selective listening. Applying the same analysis to AUD-CO interconnectivity data (Fig. 4), we found a non-significant trend for the main effect of the quadratic AUD-CO interconnectivity on response confidence (OR = 0.94, $p = 0.08$).

In comparison to the previous work, the present study is unique in three important aspects. First, the auditory task was neither a word recognition task (as in speech-in-noise experiments) nor a categorical perceptual decision-making task (e.g., absence/presence of tone). The task required the listeners to flexibly switch and maintain auditory attention on a trial-by-trial basis. Second, listeners reported their confidence in own decision on each trial simultaneously. Importantly, this subjective measure of performance was not correlated with response accuracy or speed across participants, thus providing an independent yet complementary metacognitive measure of adaptive listening behavior. Arguably, while inter-individual differences in response confidence was related to listeners' ability to aggregate information about the consecutive tones in the to-be-attended stream, differences in response speed likely reflect shifts in decision criteria (Vaden et al., 2022). Third, this is the first study that combines behavior with network neuroscience to explain individual differences in metacognitive aspects of adaptive listening behavior by dynamics of large-scale brain networks.

Limitations and future directions

Our study attempts to fill the knowledge gap on cortical substrate of individual differences in selective listening behavior under uncertainty by studying the listening brain within the functional segregation and integration framework (Power et al., 2011). We showed that during selective listening functional segregation of whole-brain network increased, a reconfiguration that entailed the auditory attentional-control network. The interconnectivity within this network was significantly modulated by task, the degree of which predicted individual differences in listening confidence. This suggests a potential role of network hubs within this network in guiding individuals' listening metacognition (cf. Gratton et al., 2017). Indeed, it has been previously suggested that control

networks do not function in isolation but rather display context-dependent dynamic interactions amongst each other in support of adaptive behaviors (Menon and D'Esposito, 2022).

Another important question is the neurophysiological basis of individual differences in metacognition during listening. Previous work from our lab provide important insights into how dynamics of low-frequency neural oscillations underlie individual differences in objective measures of selective listening behavior (Alavash et al., 2017; Wöstmann et al., 2019; Tune et al., 2021; Alavash et al., 2021). Recent studies investigating the neural correlates of metacognitive performance during perceptual decision-making suggest a link between pre-stimulus neural activity in alpha frequency band (8–12 Hz) and decision confidence (Kayser et al., 2016; Wostmann et al., 2019). Knowing the previously proposed associations between modulations in alpha oscillations and activity of cinguloopercular and dorsal attention networks (Sadaghiani and Kleinschmidt, 2016) one prediction is that alpha oscillations organize the interconnectivity dynamics found in the present study. This understanding could be best obtained using simultaneous EEG-fMRI.

Finally, the present study holds important clinical implications. Age-related hearing loss often deteriorates neural and behavioral implementation of auditory selective attention, the degree of which varies across listeners (Dai et al., 2018; Tune et al., 2021). Objective measures of listening behavior do not reveal the full spectrum of problems that the hearing impaired experiences in challenging listening situations. To understand, predict, or compensate this deficit at individual level, it is essential to find neural markers of subjective and objective measures of selective listening. There is currently little known about how hearing loss might affect the capacity to monitor or calibrate own listening behavior (i.e., listening metacognition). Our study provides the basis to address this question (or similar ones in deficits of auditory perception) on both behavioral and brain level.

To conclude, the dynamics of interconnectivity across auditory and attentional-control networks account for individual differences in metacognition during adaptive listening behavior.

Materials and Methods

Participants

Forty-five participants were invited to take part in the study. All participants were right-handed (assessed by a translated version of the Edinburgh Handedness Inventory (Oldfield, 1971)), had normal or corrected-to-normal vision, and all had normal hearing (assessed using pure tone audiometry (PTA); left-right average PTA across frequencies .025-8KHZ < 25 dbHL). None of the participants had any history of neurological or psychiatric disorders. Five participants were excluded as their data did not fulfill the criteria used to assess the quality of fMRI images (see section *FMRI data acquisition and preprocessing* below). Accordingly, 40 participants were included in the main analysis (age range = 18-32 years, median age = 23, 13 males). All procedures were in accordance with the Declaration of Helsinki and approved by the local ethics committee of the University of Lübeck. All participants gave written informed consent and were financially compensated (10€/h).

Procedure

Each imaging session consisted of seven fMRI runs (Fig. 1A): eyes-open resting state (~10 min) followed by six runs in which participants performed an adaptive selective pitch discrimination task (~10 min each) (SI Appendix has a detailed description of the stimuli and task). During each resting state and each run of the listening task, 610 and 550 functional volumes were acquired, respectively. A structural scan (~5 min) was acquired at the end of the imaging session (SI Appendix has MRI acquisition parameters). Before functional and structural imaging, outside MRI room, each

participant completed a screening procedure used to assess handedness, a shortened version of the Spatial, Speech and Hearing Quality Scale (SSQ; Gatehouse and Noble, 2004)., as well as complete pure tone and speech-in-noise audiometry in free field in a sound-attenuated cabin.

FMRI analysis

An overview of the steps undertaken to preprocess and analyze the fMRI data is provided in Fig. S1. Volumetric images acquired from each participant were converted from DICOM format to standard BIDS format (Gorgolewski et al., 2016) using HeuDiConv (Halchenko, 2018). The result of this conversion was used as the input for preprocessing using fMRIPrep (Esteban et al., 2019). At this step, minimal preprocessing was applied to the data using standard fMRIPrep procedure (see SI Appendix text for details). In addition, image quality measures were extracted from outputs of DICOM-to-BIDS conversion using MRIQC tool (Esteban et al., 2017). To control the quality of the data, we used the criteria identical to (Faskowitz et al., 2020). Specifically, functional data were excluded if more than 25% of the frames exceeded 0.2-mm framewise displacement (Parkes et al., 2018), or if marked as an outlier (exceeding 1.5×interquartile range (IQR) in the adverse direction) in more than half of the following seven image quality metrics (calculated within datasets, across all functional acquisitions): dvars, tsnr, fd mean, aor, aqi, snr and efc (see MRIQC documentation for definitions). Accordingly, five data sets and two runs of two participants were excluded from the main analysis.

Cortical parcellation. As in our previous study (Alavash et al., 2019) cortical nodes were defined using a previously established functional parcellation (Gordon et al., 2016), which has shown relatively higher accuracy compared with other parcellations (Arslan et al., 2017). This parcellation is based on surface-based resting-state functional connectivity boundary maps and encompasses 333 cortical areas. To obtain Gordon333 parcellation in subject space, we used the maTT toolbox as in (Faskowitz et al., 2020). In brief, for each participant a Gaussian classifier surface atlas was used in combination with FreeSurfer's mris_ca_label function to transfer the group average atlas to subject space based on individual surface curvature and sulcal patterns. This method rendered a T1w space volume for each participant. For use with functional data, the parcellation was resampled to 2-mm T1w space.

Nuisance regression. To minimize the effects of spurious temporal correlations induced by physiological and movement artifacts, a nuisance regression procedure was implemented using the fmri-2-mqt toolbox as in (Faskowitz et al., 2020). In this procedure, each pre-processed BOLD image is linearly de-trended, confound regressed and standardized. The confound regression employed was identical to our previous study (Alavash et al., 2019) and included six motion estimates and their first-order derivatives, time series of the mean cerebrospinal fluid, and mean white matter signal. Furthermore, a spike regressor was added for each fMRI frame exceeding a motion threshold (HCP = 0.25-mm root mean squared displacement; MSC and HBN = 0.5-mm FD). Note that global signal was not regressed out from the regional time series, as it is still an open question in the field what global signal regression in fact regresses out (Murphy and Fox, 2016; Power et al., 2017). Importantly, our main results point to the reconfiguration of an auditory attentional-control network, which does not overlap with the mainly sensorimotor disruption map of the global signal (Power et al., 2017). After pre-processing and nuisance regression, residual mean BOLD time series at each node were recovered. This processing was performed for both resting-state and listening-task data. To allow for signal equilibration, the first 10 volumes of resting state and each run of the listening task were removed.

Functional connectivity. Residual time series were band-pass filtered by means of maximum overlap discrete wavelet transform (Daubechies wavelet of length eight as implemented in waveslim R

package), and the results of the filtering within the range of 0.06–0.12 Hz (wavelet scale three) were used for additional analyses, identical to our previous work (Alavash et al., 2019). It has been previously documented that the behavioral correlates of the functional connectome are best observed by analyzing low-frequency large-scale brain networks (Zhang et al., 2016). The use of wavelet scale three was motivated by previous work showing that behavior during cognitive tasks predominately correlated with changes in functional connectivity in the same frequency range (Alavash et al., 2015b; Alavash et al., 2018). To obtain a measure of association between each pair of cortical regions, Pearson correlations between wavelet coefficients were computed, which resulted in one 333 × 333 correlation matrix per participant for each resting state and run of the listening task (Fig. S1).

Network analysis. Brain graphs were constructed from the functional connectivity matrices by including the top 10% of the connections in the graph according to the rank of their correlation strengths (van Wijk et al., 2010; van den Heuvel et al., 2017). This resulted in sparse binary undirected brain graphs at a fixed network density of 10% and assured that the brain graphs were matched in terms of density across participants, resting state, and listening task. Mean functional connectivity was calculated as the average of the upper diagonal elements of the sparse connectivity matrix for each participant. In addition, network modularity was estimated to quantify the configuration of large-scale brain networks on macroscopic level (Rubinov and Sporns, 2010) (Fig. 2A). The mathematical formalization of network modularity is provided in SI Appendix.

Statistical analysis

Behavioral data. Performance of the participants during the listening task was assessed based on a binary measure of correct pitch discrimination (response accuracy: correct/incorrect), the inverse of response time on correct trials (response speed), and a binary measure of confidence ratings (response confidence: high/low). Trials during which no response was given (within the response time window) and trials on which RT<300ms were excluded. The single-trial behavioral measures across all individual participants were treated as the dependent variable in the (generalized) linear mixed effects analysis.

Brain data. Statistical comparisons of connectivity and network modularity between resting state and listening task were based on permutation tests for paired samples (randomly permuting the rest and task labels 10,000 times). We used Cohen's d for paired samples as the corresponding effect size.

Brain-behavior models. Brain–behavior relationship was investigated within a linear mixed effects analysis framework. To this end, each of the single-trial behavioral measures (response accuracy, speed, or confidence) across all participants was treated as the dependent variable. The main predictors in the model were titrated pitch difference (i.e., tracking parameter), time-on-task (i.e., task block number: 1-6), congruency of the tone sequences (congruent vs. not congruent), location of the lateral stream (left vs. right), and the role of the lateral stream (attended vs. ignored). Since in this study, the main question is whether reconfiguration of resting-state brain networks from rest to task relates to listening behavior, we used the mean connectivity or modularity of the brain networks as the main predictors of interest. Specifically, we included the main effect of each rest and task connectivity (or modularity) and their interaction in the models as between-subject covariates. In addition, to control for activity level of each auditory, cinguloopercular, and dorsal attention network, individual mean beta estimates obtained from activation analysis (Fig. S2) and averaged within each network were similarly included in the models as between-subject covariates. Mixed effects analyses were performed in R (R Core Team) using the packages lme4 and sjPlot.

Deviation coding was used for categorical predictors. All continuous variables were Z scored. Since response accuracy and confidence are binary variables, we used a generalized linear mixed effects model with the logit as link function in these cases. In the case of response speed, the distribution of the data did not significantly deviate from normal distribution (Shapiro–Wilk test P value = 0.8). Thus, in this case, we used linear mixed effects models with the underlying distribution set to Gaussian. For all models predicting response accuracy, confidence or speed, we report P values for individual model terms that were derived using the Satterthwaite approximation for degrees of freedom. As a measure of effects size, for the model predicting accuracy or confidence, we report OR, and for response speed, we report the regression coefficient (β).

Data visualization

Brain surfaces were visualized using Connectome Workbench. Connectograms were visualized using Brain Data Viewer. Network flow diagrams were visualized in MapEquation.

Data availability

The complete dataset associated with this work, including MRI data in BIDS format, and code of network and statistical analyses will be made publicly available upon publication on Open Science platform OSF under the link to the project page https://osf.io/a9cte/.

Acknowledgement

Anne Herrmann helped acquire the fMRI data. Research was supported by German Research Foundation (DFG) - 426620060 (grant to M.A.).

References

Alavash M, Tune S, Obleser J (2019) Modular reconfiguration of an auditory control brain network supports adaptive listening behavior. PNAS 116:660-669.

Alavash M, Tune S, Obleser J (2021) Dynamic large-scale connectivity of intrinsic cortical oscillations supports adaptive listening in challenging conditions. PLoS Biol 19:e3001410.

Alavash M, Hilgetag CC, Thiel CM, Giessing C (2015a) Persistency and flexibility of complex brain networks underlie dual-task interference. Hum Brain Mapp 36:3542-3562.

Alavash M, Doebler P, Holling H, Thiel CM, Giessing C (2015b) Is functional integration of resting state brain networks an unspecific biomarker for working memory performance? NeuroImage 108:182-193.

Alavash M, Daube C, Wöstmann M, Brandmeyer A, Obleser J (2017) Large-scale network dynamics of beta-band oscillations underlie auditory perceptual decision-making. Netw Neurosci.

Alavash M, Lim SJ, Thiel C, Sehm B, Deserno L, Obleser J (2018) Dopaminergic modulation of hemodynamic signal variability and the functional connectome during cognitive performance. NeuroImage 172:341-356.

Arslan S, Ktena SI, Makropoulos A, Robinson EC, Rueckert D, Parisot S (2017) Human brain mapping: A systematic comparison of parcellation methods for the human cerebral cortex. NeuroImage 170:5-30.

Baird B, Smallwood J, Gorgolewski KJ, Margulies DS (2013) Medial and lateral networks in anterior prefrontal cortex support metacognitive ability for memory and perception. J Neurosci 33:16657-16665.

Bang D, Fleming SM (2018) Distinct encoding of decision confidence in human medial prefrontal cortex. PNAS.

Bassett DS, Sporns O (2017) Network neuroscience. Nat Neurosci 20:353-364.

Bassett DS, Wymbs NF, Porter MA, Mucha PJ, Carlson JM, Grafton ST (2010) Dynamic reconfiguration of human brain networks during learning. PNAS 108:7641-7646.

Bertolero MA, Yeo BTT, Bassett DS, D'Esposito M (2018) A mechanistic model of connector hubs, modularity and cognition. Nat Hum Behav 2:765-777.

Corbetta M, Patel G, Shulman GL (2008) The reorienting system of the human brain: from environment to theory of mind. Neuron 58:306-324.

Coste CP, Kleinschmidt A (2016) Cingulo-opercular network activity maintains alertness. NeuroImage 128:264-272.

Dai L, Best V, Shinn-Cunningham BG (2018) Sensorineural hearing loss degrades behavioral and physiological measures of human spatial selective auditory attention. PNAS 115:E3286-E3295.

De Martino B, Fleming SM, Garrett N, Dolan RJ (2013) Confidence in value-based choice. Nat Neurosci 16:105-110.
Dosenbach NU, Fair DA, Cohen AL, Schlaggar BL, Petersen SE (2008) A dual-networks architecture of top-down control. Trends in cognitive sciences 12:99-105.
Eckert MA, Teubner-Rhodes S, Vaden KI, Jr. (2016) Is Listening in Noise Worth It? The Neurobiology of Speech Recognition in Challenging Listening Conditions. Ear Hear 37 Suppl 1:101S-110S.
Eckert MA, Menon V, Walczak A, Ahlstrom J, Denslow S, Horwitz A, Dubno JR (2009) At the heart of the ventral attention system: the right anterior insula. Human brain mapping 30:2530-2541.
Erb J, Henry MJ, Eisner F, Obleser J (2013) The brain dynamics of rapid perceptual adaptation to adverse listening conditions. J Neurosci 33:10688-10697.
Esteban O, Birman D, Schaer M, Koyejo OO, Poldrack RA, Gorgolewski KJ (2017) MRIQC: Advancing the automatic prediction of image quality in MRI from unseen sites. PLoS One 12:e0184661.
Esteban O, Markiewicz CJ, Blair RW, Moodie CA, Isik AI, Erramuzpe A, Kent JD, Goncalves M, DuPre E, Snyder M, Oya H, Ghosh SS, Wright J, Durnez J, Poldrack RA, Gorgolewski KJ (2019) fMRIPrep: a robust preprocessing pipeline for functional MRI. Nat Methods 16:111-116.
Faskowitz J, Esfahlani FZ, Jo Y, Sporns O, Betzel RF (2020) Edge-centric functional network representations of human cerebral cortex reveal overlapping system-level architecture. Nat Neurosci.
Fleming SM, Dolan RJ (2012) The neural basis of metacognitive ability. Philos Trans R Soc Lond B Biol Sci 367:1338-1349.
Fleming SM, Dolan RJ, Frith CD (2012a) Metacognition: computation, biology and function. Philos Trans R Soc Lond B Biol Sci 367:1280-1286.
Fleming SM, Huijgen J, Dolan RJ (2012b) Prefrontal Contributions to Metacognition in Perceptual Decision Making. J Neurosci 32:6117-6125.
Fleming SM, Ryu J, Golfinos JG, Blackmon KE (2014) Domain-specific impairment in metacognitive accuracy following anterior prefrontal lesions. Brain 137:2811-2822.
Fox MD, Corbetta M, Snyder AZ, Vincent JL, Raichle ME (2006) Spontaneous neuronal activity distinguishes human dorsal and ventral attention systems. PNAS 103:10046-10051.
Galvin SJ, Podd JV, Drga V, Whitmore J (2003) Type 2 tasks in the theory of signal detectability: discrimination between correct and incorrect decisions. Psychonomic Bull Rev 104:843-876.
Gatehouse S, Noble W (2004) The Speech, Spatial and Qualities of Hearing Scale (SSQ). Int J Audiol 43:85-99.
Geerligs L, Rubinov M, Cam C, Henson RN (2015) State and Trait Components of Functional Connectivity: Individual Differences Vary with Mental State. J Neurosci 35:13949-13961.
Gordon EM, Laumann TO, Adeyemo B, Huckins JF, Kelley WM, Petersen SE (2016) Generation and evaluation of a cortical area parcellation from resting-state correlations. Cereb Cortex 26:288-303.
Gordon EM, Lynch CJ, Gratton C, Laumann TO, Gilmore AW, Greene DJ, Ortega M, Nguyen AL, Schlaggar BL, Petersen SE, Dosenbach NUF, Nelson SM (2018) Three distinct sets of connector hubs integrate human brain function. Cell Rep 24:1687-1695 e1684.
Gorgolewski KJ et al. (2016) The brain imaging data structure, a format for organizing and describing outputs of neuroimaging experiments. Sci Data 3:160044.
Gratton C, Sun H, Petersen SE (2017) Control networks and hubs. Psychophysiology.
Gratton C, Laumann TO, Nielsen AN, Greene DJ, Gordon EM, Gilmore AW, Nelson SM, Coalson RS, Snyder AZ, Schlaggar BL, Dosenbach NUF, Petersen SE (2018) Functional brain networks are dominated by stable group and individual factors, not cognitive or daily Variation. Neuron 98:439-452 e435.
Guggenmos M (2021) Measuring metacognitive performance: type 1 performance dependence and test-retest reliability. Neurosci Conscious 2021:niab040.
Halchenko YOea (2018) Open Source Software: Heudiconv. Zenodo.
Hebart MN, Schriever Y, Donner TH, Haynes JD (2016) The Relationship between Perceptual Decision Variables and Confidence in the Human Brain. Cereb Cortex 26:118-130.
Hill KT, Miller LM (2010) Auditory attentional control and selection during cocktail party listening. Cereb Cortex 20:583-590.
Kayser SJ, McNair SW, Kayser C (2016) Prestimulus influences on auditory perception from sensory representations and decision processes. PNAS 113:4842-4847.
Kepecs A, Uchida N, Zariwala HA, Mainen ZF (2008) Neural correlates, computation and behavioural impact of decision confidence. Nature 455:227-231.
Kiani R, Shadlen MN (2009) Representation of confidence associated with a decision by neurons in the parietal cortex. Science 324:759-764.
Lee AK, Larson E, Maddox RK, Shinn-Cunningham BG (2014) Using neuroimaging to understand the cortical mechanisms of auditory selective attention. Hearing Res 307:111-120.
Marek S, Dosenbach NUF (2018) The frontoparietal network: function, electrophysiology, and importance of individual precision mapping. Dialogues Clin Neurosci 20:133-140.
Menon V, Uddin LQ (2010) Saliency, switching, attention and control: a network model of insula function. Brain Struct Funct 214:655-667.

Menon V, D'Esposito M (2022) The role of PFC networks in cognitive control and executive function. Neuropsychopharmacology 47:90-103.
Middlebrooks PG, Sommer MA (2012) Neuronal correlates of metacognition in primate frontal cortex. Neuron 75:517-530.
Murphy K, Fox MD (2016) Towards a consensus regarding global signal regression for resting state functional connectivity MRI. NeuroImage 154:169-173.
Neta M, Schlaggar BL, Petersen SE (2014) Separable responses to error, ambiguity, and reaction time in cingulo-opercular task control regions. NeuroImage 99:59-68.
Neta M, Nelson SM, Petersen SE (2017) Dorsal Anterior Cingulate, Medial Superior Frontal Cortex, and Anterior Insula Show Performance Reporting-Related Late Task Control Signals. Cereb Cortex 27:2154-2165.
Oldfield R (1971) The assessment and analysis of handedness: The Edinburgh inventory. Neuropsychologia 9:97-113.
Parkes L, Fulcher B, Yucel M, Fornito A (2018) An evaluation of the efficacy, reliability, and sensitivity of motion correction strategies for resting-state functional MRI. NeuroImage 171:415-436.
Peelle JE (2017) Listening Effort: How the Cognitive Consequences of Acoustic Challenge Are Reflected in Brain and Behavior. Ear Hear.
Petersen SE, Posner MI (2012) The attention system of the human brain: 20 years after. Annu Rev Neurosci 35:73-89.
Posner MI (2012) Imaging attention networks. NeuroImage 61:450-456.
Power JD, Petersen SE (2013) Control-related systems in the human brain. Current Opin Neurobiol 23:223-228.
Power JD, Plitt M, Laumann TO, Martin A (2017) Sources and implications of whole-brain fMRI signals in humans. NeuroImage 146:609-625.
Power JD, Cohen AL, Nelson SM, Wig GS, Barnes KA, Church JA, Vogel AC, Laumann TO, Miezin FM, Schlaggar BL, Petersen SE (2011) Functional network organization of the human brain. Neuron 72:665-678.
Puschmann S, Steinkamp S, Gillich I, Mirkovic B, Debener S, Thiel CM (2017) The right temporoparietal junction supports speech tracking during selective listening: Evidence from concurrent EEG-fMRI. J Neurosci 37:11505-11516.
Rouault M, Lebreton M, Pessiglione M (2023) A shared brain system forming confidence judgment across cognitive domains. Cereb Cortex 33:1426-1439.
Rouault M, McWilliams A, Allen MG, Fleming SM (2018) Human metacognition across domains: insights from individual differences and neuroimaging. Personal Neurosci 1.
Rubinov M, Sporns O (2010) Complex network measures of brain connectivity: uses and interpretations. NeuroImage 52:1059-1069.
Sadaghiani S, D'Esposito M (2015) Functional Characterization of the Cingulo-Opercular Network in the Maintenance of Tonic Alertness. Cereb Cortex 25:2763-2773.
Sadaghiani S, Kleinschmidt A (2016) Brain Networks and alpha-Oscillations: Structural and Functional Foundations of Cognitive Control. Trends in cognitive sciences 20:805-817.
Seeley WW, Menon V, Schatzberg AF, Keller J, Glover GH, Kenna H, Reiss AL, Greicius MD (2007) Dissociable intrinsic connectivity networks for salience processing and executive control. J Neurosci 27:2349-2356.
Sestieri C, Corbetta M, Spadone S, Romani GL, Shulman GL (2014) Domain-general signals in the cingulo-opercular network for visuospatial attention and episodic memory. Journal of cognitive neuroscience 26:551-568.
Shiell MM, Hausfeld L, Formisano E (2018) Activity in Human Auditory Cortex Represents Spatial Separation Between Concurrent Sounds. J Neurosci 38:4977-4984.
Shinn-Cunningham B (2017) Cortical and Sensory Causes of Individual Differences in Selective Attention Ability Among Listeners With Normal Hearing Thresholds. J Speech Lang Hear Res 60:2976-2988.
Shinn-Cunningham BG (2008) Object-based auditory and visual attention. Trends in cognitive sciences 12:182-186.
Szczepanski SM, Pinsk MA, Douglas MM, Kastner S, Saalmann yB (2013) Functional and structural architecture of the human dorsal frontoparietal attention network. PNAS 110:15806-15811.
Tune S, Alavash M, Fiedler L, Obleser J (2021) Neural attentional-filter mechanisms of listening success in middle-aged and older individuals. Nat Commun 12:4533.
Uddin LQ (2015) Salience processing and insular cortical function and dysfunction. Nat Rev Neurosci 16:55-61.
Vaccaro AG, Fleming SM (2018) Thinking about thinking: A coordinate-based meta-analysis of neuroimaging studies of metacognitive judgements. Brain Neurosci Adv 2:2398212818810591.
Vaden KI, Jr., Eckert MA, Dubno JR, Harris KC (2019) Cingulo-opercular adaptive control for younger and older adults during a challenging gap detection task. J Neurosci Res.
Vaden KI, Jr., Teubner-Rhodes S, Ahlstrom JB, Dubno JR, Eckert MA (2022) Evidence for cortical adjustments to perceptual decision criteria during word recognition in noise. NeuroImage 253:119042.
Vaden KI, Jr., Kuchinsky SE, Cute SL, Ahlstrom JB, Dubno JR, Eckert MA (2013) The cingulo-opercular network provides word-recognition benefit. J Neurosci 33:18979-18986.

van den Heuvel M, de Lange S, Zalesky A, Seguin C, Yeo T, Schmidt R (2017) Proportional thresholding in resting-state fMRI functional connectivity networks and consequences for patient-control connectome studies: Issues and recommendations. NeuroImage 152:437-449.

van Wijk BCM, Stam CJ, Daffertshofer A (2010) Comparing Brain Networks of Different Size and Connectivity Density Using Graph Theory. PloS one 5:e13701.

Vossel S, Geng JJ, Fink GR (2014) Dorsal and ventral attention systems: distinct neural circuits but collaborative roles. The Neuroscientist 20:150-159.

Waschke L, Wostmann M, Obleser J (2017) States and traits of neural irregularity in the age-varying human brain. Sci Rep 7:17381.

Wild CJ, Yusuf A, Wilson DE, Peelle JE, Davis MH, Johnsrude IS (2012) Effortful listening: the processing of degraded speech depends critically on attention. J Neurosci 32:14010-14021.

Wostmann M, Waschke L, Obleser J (2019) Prestimulus neural alpha power predicts confidence in discriminating identical auditory stimuli. Eur J Neurosci 49:94-105.

Wostmann M, Erb J, Kreitewolf J, Obleser J (2021) Personality captures dissociations of subjective versus objective hearing in noise. R Soc Open Sci 8:210881.

Wöstmann M, Alavash M, Obleser J (2019) Alpha Oscillations in the Human Brain Implement Distractor Suppression Independent of Target Selection. J Neurosci 39:9797-9805.

Zhang Z, Telesford QK, Giusti C, Lim KO, Bassett DS (2016) Choosing Wavelet Methods, Filters, and Lengths for Functional Brain Network Construction. PloS one 11:e0157243.